SUPPLEMENTARY INFORMATION

Specific evidence of low-dimensional continuous attractor dynamics in grid cells

KiJung Yoon[1], Michael A. Buice[1], Caswell Barry[2,3,4], Robin Hayman[4], Neil Burgess[2,3], and Ila Fiete[1]

[1]Center for Learning and Memory, University of Texas at Austin, Austin, TX 78712, USA.
[2]Institute of Cognitive Neuroscience, University College London, 17 Queen Square, London WC1N 3AR, UK.
[3]Institute of Neurology, University College London, 17 Queen Square, London WC1N 3BG, UK.
[4]Institute of Behavioural Neuroscience, Division of Psychology and Language Sciences, University College London, 26 Bedford Way, London WC1H 0AP, UK.

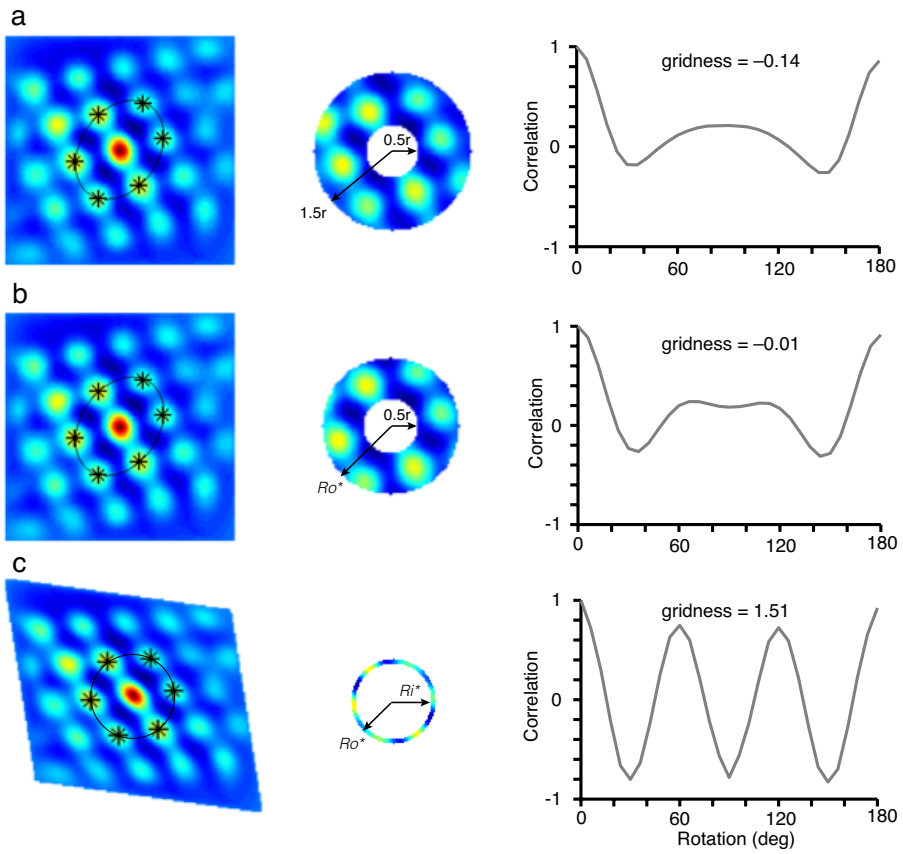

Figure S1: **Standard and modified (our method) gridness scores for anisotropic (non-equilateral) triangular grid cell responses. (a)** Left: A sample autocorrelogram is characterized by a non-equilateral triangular lattice. The nearest six local peaks (black asterisks) are circumscribed by the best-fit (black) ellipse. Middle: An annulus containing the nearest six local peaks ($R_i = 0.5r, R_o = 1.5r$; r is the average distance from the center to the six nearest peaks). Right: The Pearson correlation between the indicated annulus and the same annulus rotated by an angle in the interval $[0, \pi]$ as a function of angle. Gridness score is marked above the curve. **(b)** Left: the autocorrelogram (as in a). Middle: a choice of annulus with R_i fixed at $0.5r$ and where R_o is increased from $r + 1(cm)$ in steps of $1(cm)$. R_o^* is chosen as the value that produces the maximum gridness score ($= 0.01$). Right: As above. **(c)** Left: The transformed autocorrelogram with the six nearest peaks circumscribed by a circle. Middle: The annulus that resulted in the maximum gridness score (=1.51) over the set of annuli with $R_i \in [0.5r, r]$ and $R_o \in [r + 1, 1.5r]$. Right: As above.

Figure S2-1

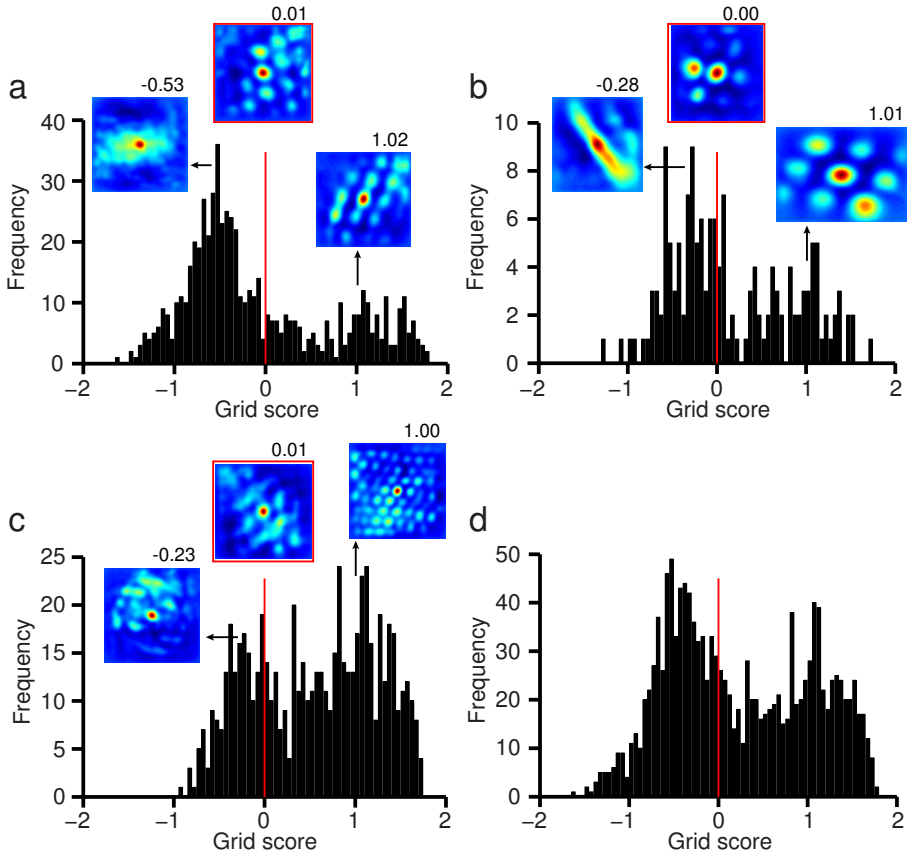

Figure S2-2

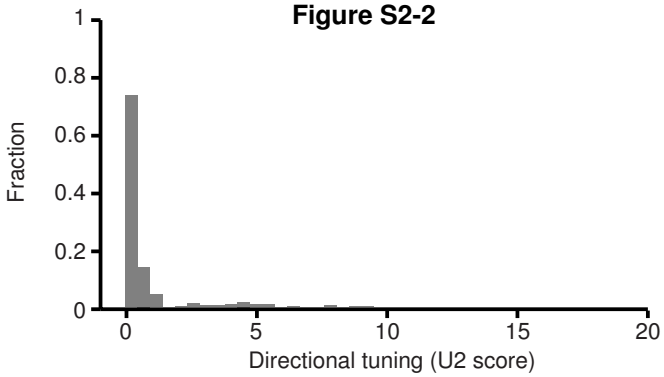

Figure S2-1: **Frequency distribution of modified gridness/U2 scores for the entire sample of MEC cells from the datasets analyzed in this paper. (a)** Cells from **Figs. 1, 2,** and **7**; **(b)** cells from **Fig. 3**, and **(c)** cells from **Figs. 4** and **5**. The red line indicates our gridness threshold, which is equal to zero. Insets show spatial autocorrelograms of cells that represent non-grid cells (peak of the distribution on the left of the threshold), cells whose gridness score is close to the threshold, and cells above threshold (with a gridness score around 1.0). **(d)** The combined distribution of gridness scores for all previous samples. Note: Many cells in **a** were recorded from deep layers (III, V, VI) of MEC, and had grid scores lower than threshold.

Figure S2-2: Histogram of head-directional tuning for all cells in **Supplementary Fig. 2-1a** that obtained higher grid score than the threshold. Directional tuning is expressed by Watson's U2 score.

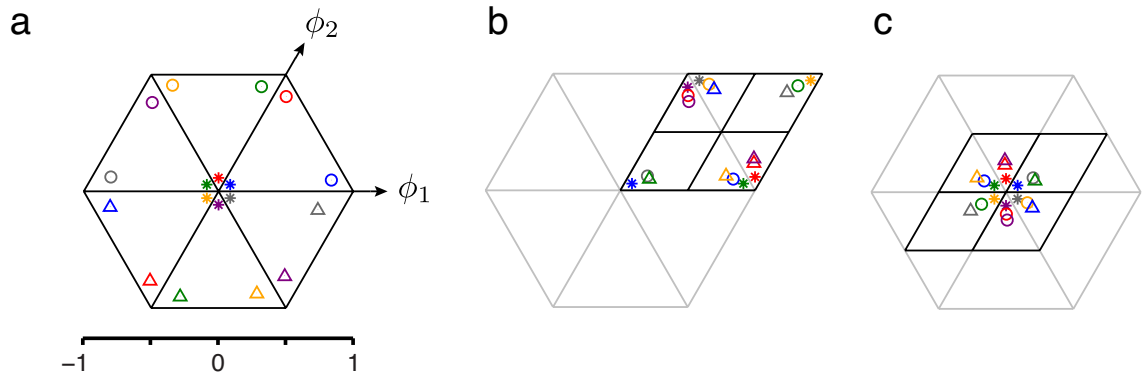

Figure S3: **Periodicity of the phase variable and how phase is computed.** Exemplar spatial phases adjacent to zero in **(a)** regular hexagonal unit cell, **(b)** rhomboidal unit cell mapped from **a** through mod 1, and **(c)** rhomboidal unit cell ranging from 0.5 to 0.5 by remapping phases in **b** to the origin. Each distinct symbol and color represents an identical spatial phase across transformed unit cells. Note that phases distant from the origin approximately by one grid period (circles and triangles) in **a** are mapped into the neighborhood of origin in **c**.

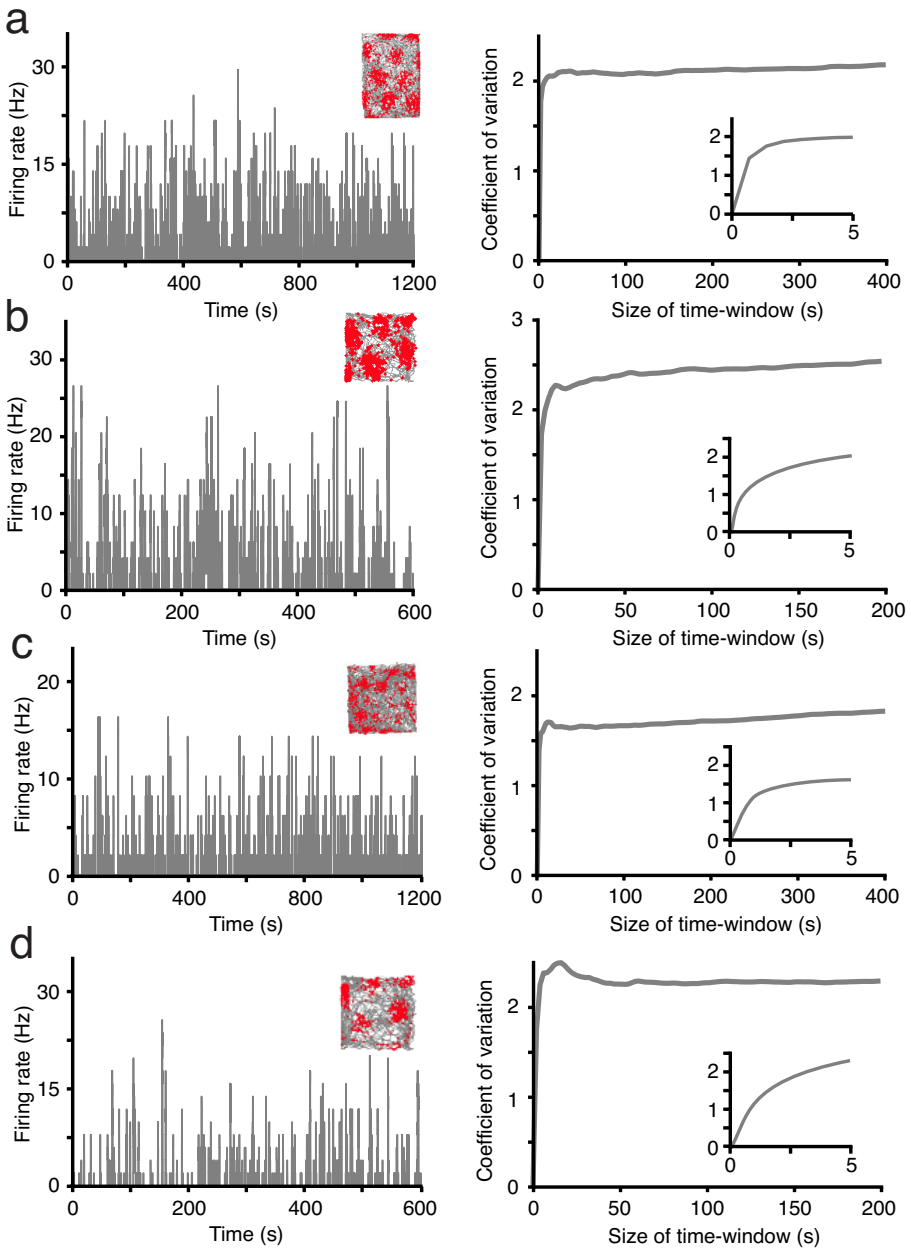

Figure S4: **Mean-corrected coefficient of variation (CV) analysis to assess the stochasticity of grid cell spike trains.** Left column: The time-varying firing rates of some example grid cells (N=4; inset), generated by sliding a window over each cell's spike train. The window is a boxcar (i.e., zero everywhere except for the interval $[t, t+\Delta t)$, where it is one; Δt is the window length and t is slid from $t = 0$ to $T - \Delta t$, where T is the length of the recording). Shown is the firing rate computed with $\Delta t = 0.5$ sec. Right column: Coefficient of variation (CV) for the interspike intervals, with spike times rescaled according to a windowed firing rate (as in Left), as a function of window size (see Online Methods). Inset: magnified representation of CV for windows lengths of 0 to 5 seconds. Note that the CV exceeds 1 for all cells for windows of length 600 ms and greater, and is considerable in size (exceeds 0.5) even for windows of length 300 ms. (ref 1: Softky, W. R. & Koch, C. The highly irregular firing of cortical cells in inconsistent with temporal integration of random EPSPs. *J. Neurosci.* **13**, 334350 (1993). ref 2: Shadlen, M. N. & Newsome, W. T. Noise, neural codes and cortical organization. *Curr. Opin. Neurobiol.* **4**, 569-579 (1994)).

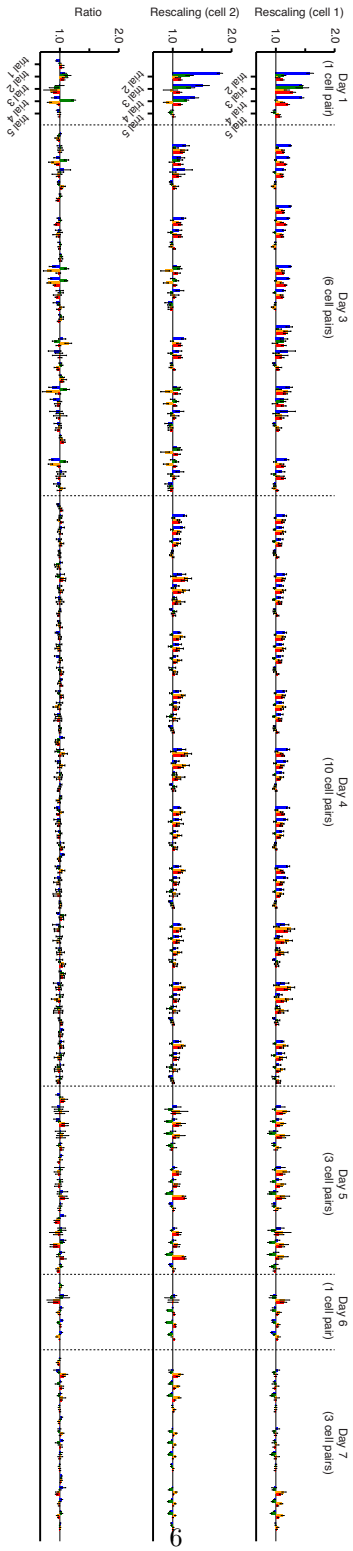

Figure S5: **A summary of all cell pairs in novel environments, analyzed as in Fig. 4c-e.** Color scheme as in **Figs. 3c** and **4d,e**. Grid parameters for sets of cells (top: cell 1; middle: cell 2) normalized to the corresponding value on the first trial of the day (familiar environment), and ratio between the corresponding cells (aligned vertically) of each grid parameter for each trial (bottom) across all 24 cell pairs. Each day shows a set of parameters for cells recorded that day, similar to those in **Fig. 3c,d** (e.g. day 3 has 6 cell pairs and six groups of parameters; the recorded cells on different days are different, but from the same area of one animal). A few trials are omitted due to the low gridness score of the cell's response. Note that "cell 1" and "cell 2" are not specific cells, i.e. each row does not represent the same cell across days; however, each column does represent the same cell *pair*.

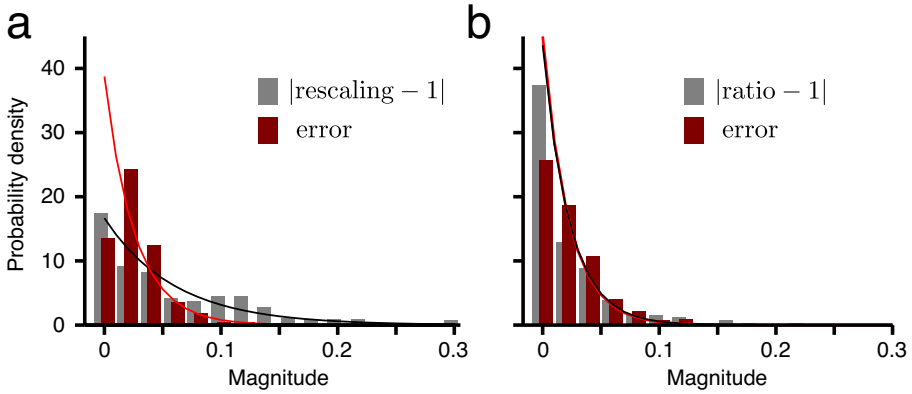

Figure S6: **Stable grid parameter ratios even when grids are rescaled.** **(a)** Histogram (normalized) of grid parameter rescalings (i.e., grid parameter ratios for each parameter and each cell, taken across time/trials) for all cells in **Fig. 3f** (gray), with a normalized histogram of error magnitudes for each measurement (red). Parameter rescalings are plotted by subtracting one, and taking the absolute value, to compare against error magnitudes. Solid lines: best-fit exponential distributions ($\alpha \cdot e^{\alpha x}$). The width $1/\alpha_{data}$ of the parameter rescaling distribution is significantly larger than the width $1/\alpha_{null}$ of the error distribution ($\alpha_{data} < \alpha_{null}; P \ll 10^{-4}$, F-test for equality of variances of two samples). **(b)** Grid parameter ratios across time for all cell *pairs* (i.e., the ratio taken across time/trials of the ratio between cells of each parameter and each cell pair) from **Fig. 3f**: here, the width of the two distributions is not significantly different: α_{data} is not significantly different from α_{null} ($P = 0.57 \gg 0.05$, F-test for equality of variances of two samples), showing that the grid parameter ratios between neighboring cell pairs remain significantly close to one.